ICSV19
Vilnius, Lithuania
July 08-12, 2012

MATRIX-FREE CONTINUATION OF LARGE THERMOACOUSTIC SYSTEMS

Iain Waugh, Simon Illingworth and Matthew Juniper

Cambridge University Engineering Department, Cambridge, CB2 1PZ, United Kingdom, e-mail: icw26@cam.ac.uk

To define the safe operating region of a thermoacoustic system, it is critical to find the regions of parameter space where limit cycles exist. Continuation methods allow limit cycles to be numerically found in the time domain, and can track the changes in the limit cycles as the operating condition of the thermoacoustic system changes.

Most continuation methods for finding limit cycles are impractical for large thermoacoustic systems, because the computational time and memory required to form the Jacobian matrices is too large. There are thus only a few applications in the literature of continuation methods for thermoacoustic systems, all with low-order models.

Matrix-free shooting methods are effective for calculating the limit cycles of dissipative systems and have been demonstrated recently in fluid dynamics, but are yet unused in thermoacoustics. The matrix-free methods converge quickly to limit cycles by implicitly using a 'reduced order model' property; the iterative methods preferentially use the important bulk motions of the system, whilst ignoring features that are quickly dissipated in time. The matrix-free methods are demonstrated on a model of a ducted 2D diffusion flame, and the stability limits are calculated across a parameter range. Both subcritical and supercritical Hopf bifurcations are found. Physical information about the flame-acoustic interaction is found from the mode shape of limit cycles.

1. Introduction

Thermoacoustic oscillations can occur whenever combustion takes place inside an acoustic resonator. Unsteady combustion is an efficient acoustic source, and combustors tend to be highly resonant systems. Therefore for suitable phase differences between combustion and acoustic perturbations, large-amplitude self-excited limit cycles can occur. Because limit cycles are generally unwanted in a combustion system, we are interested in finding the safe operating region of parameter space, where no limit cycles (or other high-amplitude states such as chaos) exist.

Nonlinear analyses are required in order to calculate limit cycle amplitudes and mode shapes, and to quantify the extent of any bistable operating regions. In thermoacoustics, it is common to see a branch of limit cycles emerging from a Hopf bifurcation. A Hopf bifurcation is where a complex pair of eigenvalues of the Jacobian matrix (for the fixed point) have zero real part. Hopf bifurcations in thermoacoustics are either supercritical or subcritical, as shown schematically in Figure 1(a) and (b). Both types of bifurcation have been seen in experimental combustors [1]. When subcritical Hopf bifurcations are present in a system, triggering can occur from a linearly stable fixed point to a large amplitude limit cycle. The triggering can be instigated by a pulse [2] or the action of background or combustion noise [3].

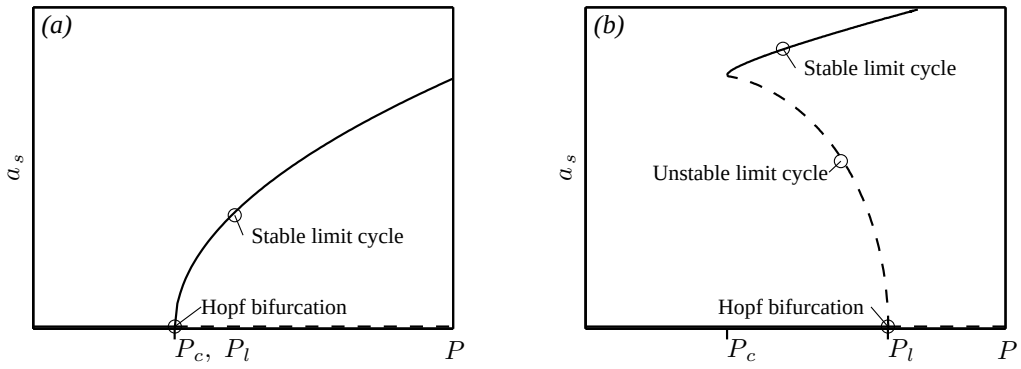

Figure 1: Schematic supercritical (a) and subcritical (b) Hopf bifurcations, in terms of the limit cycle amplitude, a_s and a system parameter P. The critical parameter, P_c, is the parameter value where limit cycles first occur. The linear stability limit, P_l, is the same as the Hopf bifurcation point. In the subcritical Hopf bifurcation, there is a bistable region where there is both a stable fixed point and a stable limit cycle ($P_c < P < P_l$). Triggering can occur in the bistable region.

In the time domain, continuation analysis has been developed in the field of nonlinear dynamics to track solutions whilst varying system parameters. The solutions can be fixed points, limit cycles, or bifurcations. A summary of relevant bifurcations in fluid dynamics is given in Cliffe [4]. Software packages are available for continuation of systems with $\mathcal{O}(10)$ variables, and have been applied to simple thermoacoustic systems [8, 9, 10]. The methods applied in these papers, however, are impractical for larger systems because they use direct solvers for the underlying linear algebra. Continuation analysis relies on the solution of a series of linear equations to find solutions, and the exact solution of these linear equations becomes prohibitively expensive for larger systems, both in terms of computational time and memory usage.

Matrix-free iterative methods can reduce both the computational time and memory usage during the solution of the linear equations. Matrix-free methods have recently been used to find cusp bifurcations [5] and limit cycles in thermal convection [6], with $\mathcal{O}(10^3)$ variables. Limit cycles have also been extracted from turbulent Couette flow [7] with $\mathcal{O}(10^5)$ variables, using matrix-free methods and hook-step optimisation routines.

The dissipative nature of fluid systems means that matrix-free methods are particularly well suited to finding limit cycles. Because combustion and fluids systems are dissipative, only a few bulk fluid motions are important in the long time limit, and therefore there are far fewer important degrees of freedom than there are variables. The iterative methods inexactly solve the linear equations by implicitly using these important bulk motions, whilst ignoring features that are quickly dissipated in time.

The aim of this paper is to present a method for finding limit cycles in large thermoacoustic models, using an iterative matrix-free continuation technique (further details in [16]). The technique is able to calculate the safe operating region of the thermoacoustic system in the time domain, and find the mode shape and frequencies of any limit cycles. The paper begins by introducing the shooting methods and the iterative techniques used to converge to the limit cycles. The paper then describes how the iterative process can be achieved with matrix-free techniques. The numerical methods are then demonstrated on a model of a 2D diffusion flame in an acoustic duct in section 4.

2. Shooting to find limit cycles

Continuation analysis examines nonlinear systems with evolution:

$$\frac{\mathrm{d}\underline{x}(t)}{\mathrm{d}t} = F(\underline{x}(t), \lambda), \quad \underline{x}(t) \in \mathbb{R}^N \tag{1}$$

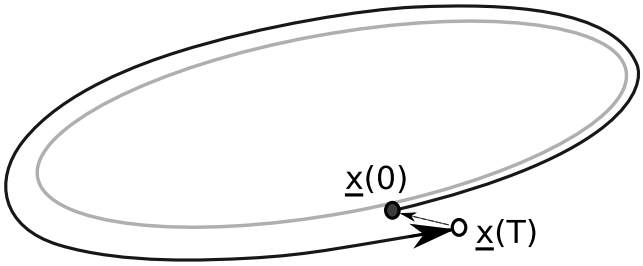

Figure 2: Shooting method to find a limit cycle. Given a current guess for a point on a limit cycle, $\underline{x}(0)$, we timemarch forward T time units to $\underline{x}(T)$, where T is our guess for the period. We then iterate our starting guess, $\underline{x}(0)$, to minimise the length of the residual vector, $\underline{x}(0) - \underline{x}(T)$, (dashed arrow).

where $\underline{x}$ is the current state of the system and λ are parameters. The governing equations are in most cases derived from the discretisation of a PDE.

When solving for limit cycles the condition is:

$$\underline{x}(0) = \underline{x}(T)\,, \quad \left\{T \in \mathbb{R}^+ | T \neq 0\right\}, \tag{2}$$

where T is the period of the orbit.

The shooting method used in this paper finds, by iteration, a state on the limit cycle, $\underline{x}(0)$, and the period of the limit cycle, T. The magnitude of the residual vector, $\underline{r} = \underline{x}(0) - \underline{x}(T)$ (Fig. 2), is reduced to a predefined tolerance by a two-step iteration process. First, we consider the evolution of the system when started from small perturbations around our current guess $[\underline{x}(0), T]$. We generate a $(N+1) \times (N+1)$ Jacobian matrix, which relates a general small change in $[\underline{x}(0), T]$ to the resulting change in $[\underline{x}(0) - \underline{x}(T), T]$. Second, we solve a linear equation with the Jacobian matrix to find the $[\underline{\Delta x}, \Delta T]$ that we should add to our current guess, $[\underline{x}(0), T]$, in order to improve the guess. If the magnitude of the residual is still too large, we repeat the first step from the improved guess.

The linear equation is shown in Equation (3) for the n^{th} iteration, where i and j are the row and column indices of the matrix [11]. It has the standard form for multi-dimensional Newton iteration, $J\underline{\Delta x} = -\underline{r}$.

$$\overbrace{\begin{bmatrix} I - M & \underline{b} \\ \underline{c} & d \end{bmatrix}}^{(N+1)\times(N+1)} \overbrace{\begin{bmatrix} \Delta\underline{x} \\ \Delta T \end{bmatrix}}^{(N+1)\times 1} = - \overbrace{\begin{bmatrix} (\underline{x}(0) - \underline{x}(T))^n \\ \theta^n \end{bmatrix}}^{(N+1)\times 1} \tag{3}$$

$$\overset{N\times N}{M_{i,j}} = \frac{\partial \underline{x}_i(T)}{\partial \underline{x}_j(0)},\ \overset{N\times 1}{\underline{b}_i} = \frac{\partial \underline{x}_i(T)}{\partial T},\ \overset{1\times N}{\underline{c}_j} = \frac{\partial \theta}{\partial \underline{x}_j(0)},\ \overset{1\times 1}{d} = \frac{\partial \theta}{\partial T}$$

$$\underline{x}(0)^{n+1} = \underline{x}(0)^n + \Delta\underline{x}, \qquad T^{n+1} = T^n + \Delta T$$

There is an infinite number of points on the limit cycle that satisfy $\underline{r} = 0$, however, so a phase condition (θ) is required to provide a unique solution state by fixing the phase of the limit cycle. For a limit cycle in a thermoacoustic system, a suitable phase condition can be that the instantaneous acoustic pressure in the fundamental mode is zero, or that the instantaneous acoustic pressure at a set location x/L of the combustor is zero. Where multiple acoustic modes are important, the value x/L should be irrational.

The j^{th} column of the Jacobian matrix can be found by perturbing $\underline{x}_j(0)$, then timemarching forward and seeing the resultant change in $\underline{x}(T)$. To fill the Jacobian matrix for each linear equation, N time-marches are required. For large thermoacoustic systems, with $\mathcal{O}(10^3)$ variables, it is impractical to form the Jacobian matrices, because the computational expense of timemarching is too high. This is the primary driver for the use of matrix-free methods.

3. Matrix-free methods

As stated in the previous section, when finding limit cycles by shooting methods the formation of the Jacobian matrix requires N timemarches, which is unfeasible for large thermoacoustic systems. Matrix-free methods are those that solve the linear equation $J\underline{\Delta x} = -\underline{r}$, without ever requiring the matrix J to be explicitly defined. The methods are iterative and only require matrix-vector products, i.e. $J\underline{v}$, where $\underline{v}$ is an arbitrary vector. This differs from many conventional methods of solving linear equations, where the matrix J is defined and then decomposed.

3.1 GMRES

The matrix-free method used in this paper for solving $J\underline{\Delta x} = -\underline{r}$ is the Generalised Minimal Residual method (GMRES) [12]. GMRES uses k matrix-vector products to define a k-dimensional Krylov subspace:

$$\mathcal{K}_k = \text{span}\left\{\underline{r}_0, J\underline{r}_0, J^2\underline{r}_0, J^3\underline{r}_0, ..., J^{k-1}\underline{r}_0\right\},$$

where $\underline{r}_0 \equiv -\underline{r} - J\underline{x}_0$, and $\underline{x}_0$ is an initial solution guess, often taken as the right hand side, $-\underline{r}$.

The vectors $\underline{r}_0, J\underline{r}_0, J^2\underline{r}_0...$ become almost linearly dependent, so the standard Arnoldi method is used to find orthonormal vectors, $\underline{q}_1, .., \underline{q}_k$, that span the Krylov subspace $\mathcal{K}_k$. Modified Gram-Schmidt methods with re-orthogonalisation are generally used to orthonormalise the vectors for large systems, because the standard Gram-Schmidt process suffers from numerical problems with large N. In each Krylov subspace, the current guess for the solution, $\underline{\Delta x}_k$, is changed to minimise the residual:

$$\text{res}_k = ||-\underline{r} - J\underline{\Delta x}_k||$$

If convergence occurs, where $\text{res}_k < \epsilon_{conv}$, the iterative procedure stops. If $\text{res}_k > \epsilon_{conv}$, another matrix-vector product is taken to form $\mathcal{K}_{k+1}$. Another Arnoldi step is taken, to add another orthogonal direction $\underline{q}_{k+1}$. The residual is then minimised in this extra direction. The vectors $\underline{q}_1, .., \underline{q}_k$ are unchanged in $\mathcal{K}_{k+1}$, so the convergence of the GMRES method is monotonic.

3.2 Finite difference matrix-vector products

Matrix-free methods solve the equation $J\underline{\Delta x} = -\underline{r}$ using only matrix-vector products. In the case of the Jacobian matrix the matrix-vector product can be approximated by finite differences, because the Jacobian matrix is formed of partial derivatives. The mapping operator, A, which represents the time marching process, is defined as:

$$\underline{x}(T) = A\left(\underline{x}(0)\right)$$

Therefore because the spatial part of the Jacobian matrix is defined in equation (3) as shown in equation (4),

$$J_{ij} = \frac{\partial\left(\underline{x}_i(0) - \underline{x}_i(T)\right)}{\partial \underline{x}_j(0)} \tag{4}$$

then the matrix-vector product for arbitrary vector $\underline{v}$ can then be approximated by equation (5), where δ is small.

$$J\underline{v} = \underline{v} - \frac{A(\underline{x}(0) + \delta\underline{v}) - A(\underline{x}(0))}{\delta} + \mathcal{O}(\delta) \tag{5}$$

To evaluate each matrix-vector product during the GMRES solution therefore requires one timemarch. The phase (θ) components of the Jacobian matrix are also partial differentials, and can similarly be used in the finite difference approach. Finite difference matrix-vector products are simple to evaluate, but care must be taken to ensure that there is adequate scaling between variables in the state vector or numerical problems may arise.

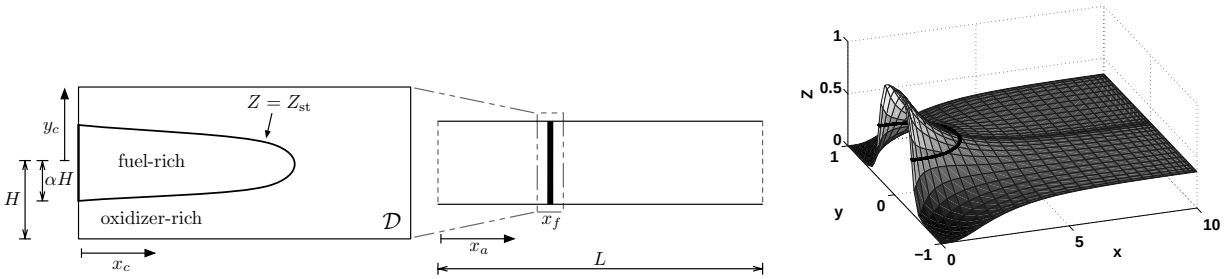

(a) The flame and duct geometry

(b) 2D steady state Z field.

Figure 3: A 2D mixture fraction field (Z) is used to describe the diffusion flame. The flame lies on the $Z = Z_{st}$ contour, which is shown as a black line in (a) and (b). The heat release from the diffusion flame domain acts at location x_f in a 1D open ended duct.

4. Ducted 2D diffusion flame model

The continuation routines are applied to a model of a thermoacoustic system containing a ducted 2D diffusion flame, first used by [13, 14] and later adapted by Illingworth to improve the accuracy by using a spectral discretisation [17]. The model contains a 2D flame domain, where the mixture fraction, Z, is discretised on a Chebyshev grid, with an axis of symmetry along the centreline. The mixture fraction obeys the non-dimensional diffusion and advection governing equation, and is specified to be $Z = 1$ in the fuel pipe ($0 < |y| < \alpha$) and $Z = 0$ in the oxidiser pipe ($\alpha < |y| < 1$), with boundary conditions $\partial Z/\partial y|_{+1,-1} = 0$, $\partial Z/\partial x|_{x_c \to \infty} = 0$. The flame lies on the contour $Z = Z_{st}$, and is assumed to have an infinite reaction rate. The location of the flame is denoted f^+.

The heat release from the model is coupled to a simple linear acoustic model of a duct [14, 9], where u and p are the nondimensional velocity and pressure pertubations in the duct. For the perturbation state, $\underline{x} = [u, p, z]$, the non-dimensional governing equations are shown below, where the subscript f denotes that the value is taken at the flame position, a bar refers to a mean quantity. The system has non-dimensional parameters: Peclet number Pe, the acoustic damping ζ, the stoichiometric mixture fraction Z_{st}, the flame position in the duct x_f, the fuel pipe width α, and the coupling parameter β_T, defined by $\beta_T = 2/(T_{inlet} - T_{adiabatic})$.

$$
\begin{aligned}
\frac{\partial u}{\partial t} &= -\frac{\partial p}{\partial x} \\
\frac{\partial p}{\partial t} &= -\frac{\partial u}{\partial x} - \zeta p \ldots \\
&\qquad + \frac{2\beta_T}{1 - Z_{st}} \delta\left(x - x_f\right) \left(- \int \int_0^{f^+} \frac{\partial z}{\partial t}\, dy dx + u_f \int_0^{\bar{f}^+} \left(\bar{Z} - Z_{st}\right) dy \right) \\
\frac{\partial z}{\partial t} &= -\bar{u}_f \frac{\partial z}{\partial x} + \frac{1}{Pe} \left(\frac{\partial^2}{\partial x^2} + \frac{\partial^2}{\partial y^2} \right) z - u_f \frac{\partial \bar{Z}}{\partial x} - u_f \frac{\partial z}{\partial x}
\end{aligned}
$$

A more complete description of the model is included in [17]. The results in this paper are generated with a 30×16 symmetric flame grid and 20 acoustic modes, giving a total system dimension of 475 (the boundary values of the Chebyshev grid are defined by the boundary conditions so are not included in this number). The model is timemarched in FORTRAN using the standard Runge-Kutta 4 technique with a timestep of 10^{-3}. The results of the model have been compared against those generated with a finer Chebyshev grid and a finer timestep, with only a 1% difference in heat release fluctuation observed.

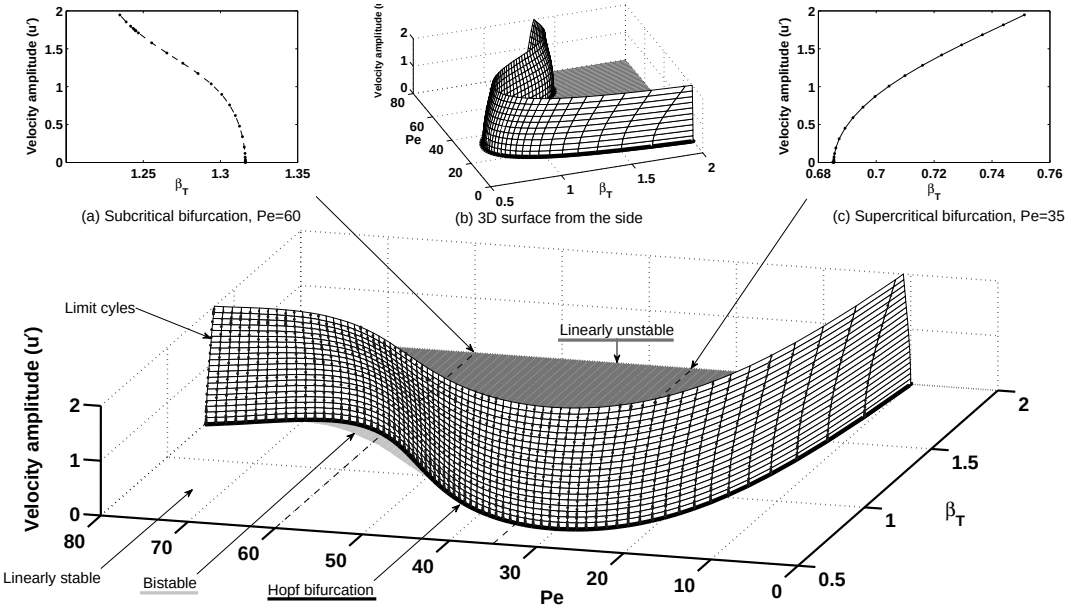

Figure 4: Continuation results for limit cycle amplitudes. The thick dark line is the Hopf bifurcation, which is the same as the linear stability limit. The linearly unstable region is shaded dark gray and the bistable region is shaded light gray (the bistable region is the vertical shadow of the subcritical bifurcation). Limit cycles are shown as dark dots on a surface interpolated between neighbouring slices. The surface exhibits both subcritical bifurcations (a) and supercritical bifurcations (c), where stable limit cycles are shown with a solid line and unstable limit cycles with a dashed line.

5. Numerical results

The next subsections show some of the physical results available from the continuation method applied to the ducted diffusion flame model. Further physical examination of the results is found in [17], and further examination of the numerics is found in [16].

5.1 Limit cycle surface

Figure 4 shows the limit cycle amplitudes as two parameters are varied: Peclet number, which changes the ratio of advection to diffusion in the flame, and β_T , which controls the extent to which unsteady combustion perturbs the acoustics (Eq. (7a)). The parameters that are held fixed are $Z_{st} = 0.8$, $c_1 = 0.0247$, $c_2 = 0.018$, $\alpha = 0.35$, $x_f = 0.25$, ${}^{ML}/_{H} = 1$. The damping coefficients are typical for a laboratory scale combustor, and $Z_{st} = 0.8$ corresponds to a diluted methane fuel and pure oxygen [15, p.94]. Each limit cycle is calculated to a tolerance of $||\underline{x}(0) - \underline{x}(T)|| < 10^{-8}$. The Hopf bifurcation marks the boundary between linearly stable and linearly unstable operating conditions. The limit cycles form a surface which has both subcritical bifurcations for $50 < Pe < 70$ (Fig. 4a) and supercritical bifurcations for $Pe < 50,\ Pe > 70$ (Fig. 4c). Where there is a subcritical bifurcation, there is a stable limit cycle at higher velocity amplitudes. However, this stable limit cycle has velocity amplitude greater than 2 and is not shown in the figure. The bistable operating conditions are those at which the system has both a stable fixed point and a stable limit cycle.

The limit cycles describe the behaviour of the fully coupled system, and are calculated by continuation analysis quite cheaply: the Hopf bifurcation line takes roughly 500s and the surface of limit cycles takes 61 CPU hours. The surface is composed of 70 slices and roughly 2500 converged limit cycles, requiring an average of 52 minutes per slice, and 90 seconds per limit cycle. A lower resolution surface can be calculated in less than 10 CPU hours, with 15 slices and coarser spacing between limit cycles. The computation can be easily parallelized because the surface is composed of separate two-dimensional slices.

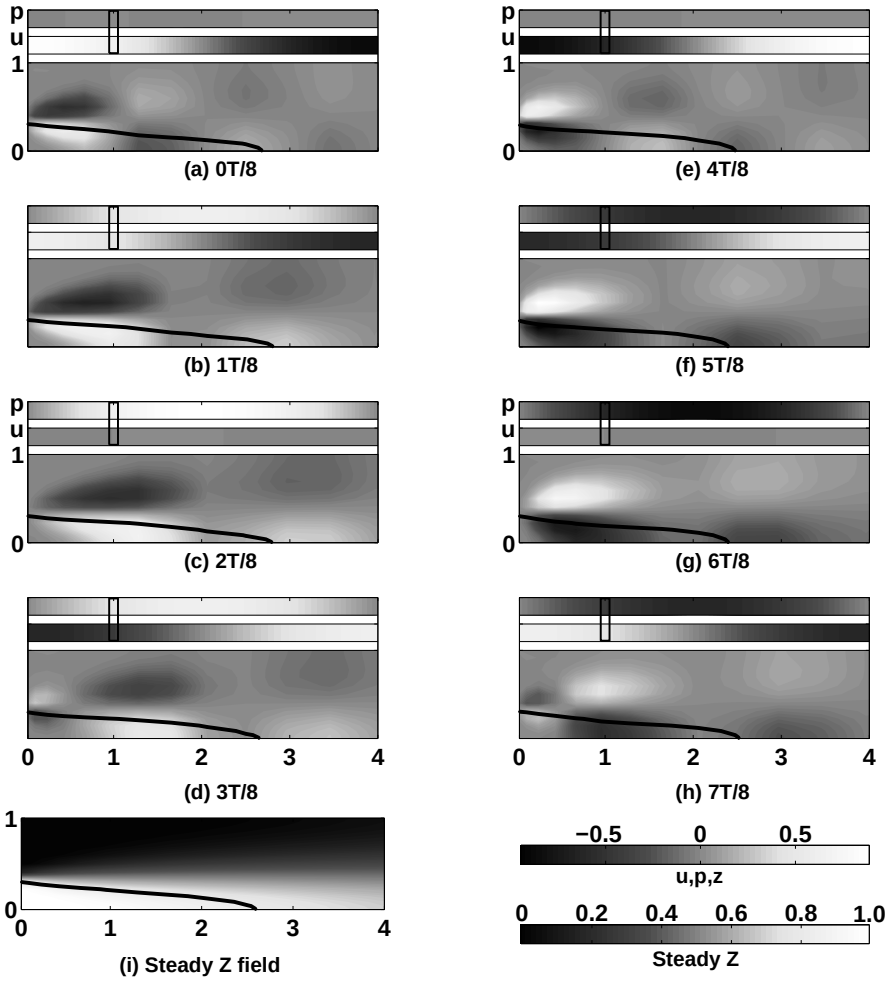

Figure 5: Snapshots of an unstable limit cycle at Pe=60, with velocity amplitude 0.62. In each snapshot (a-h), the top two bars show the perturbation pressures and velocities in the 1D duct ($x_a = 0 \rightarrow 1$), the lower bar shows the 2D perturbation z field and current flame location (black line) in the first part of the flame field ($x_c = 0 \rightarrow 4$). The flame location is marked by the black box at $x_a = 0.25$. The z values are scaled by a factor of 15 to share the colourbar with the acoustic perturbations. The steady Z field is shown in (i) for comparison.

5.2 Limit Cycles

The continuation analysis efficiently finds limit cycles, which can then be used to understand the underlying coupled flame-acoustic interaction. Figure 5 shows snapshots of the system during an unstable limit cycle, with Pe=60 and velocity amplitude 0.62. When the velocity perturbation at the flame is positive, 5(a)-(c), the flame becomes longer and, near the inlet, the regions of high and low z are stretched. When the velocity perturbation at the flame becomes negative, 5(d)-(f), the flame becomes shorter and, near the inlet, new regions of high and low z are formed. In turn, these new regions are then stretched and convected down the flame. For this limit cycle, the length of the flame only varies by $\Delta x_c \approx 0.4$ during the cycle, but slight wrinkling of the flame surface can be seen as the regions of high and low z are convected down the flame. The limit cycle has an almost symmetric form during the first and second halves of the limit cycle, which demonstrates that the nonlinearity in this flame model is weak.

6. Conclusions

Matrix-free continuation analysis can calculate limit cycles efficiently for thermoacoustic systems with coupled flame-acoustic interaction. Continuation analysis can track the limit cycles and bifurcations of the system as parameters vary, in order to find the stability limits of the system over a wide parameter range.

The dissipative nature of thermoacoustic and fluids systems makes them particularly suitable for matrix-free continuation with GMRES, because the number of important bulk motions of the system is in general much less than the total system dimension.

The continuation algorithms are used to generate a surface of limit cycles for the ducted diffusion flame, with only modest computational time. Both subcritical and supercritical Hopf bifurcations are found. The mode shapes of the limit cycles are given directly by the continuation algorithm. The mode shapes give physical insight into the nature of the coupled flame-acoustic interaction.

REFERENCES

[1] L. Kabiraj, A. Saurabh, P. Wahi, R. I. Sujith, Experimental study of thermoacoustic instability in ducted premixed flames: periodic , quasi-periodic and chaotic oscillations, *n3l- Int'l Summer School and Workshop on Non-Normal and Nonlinear Effects in Aero- and Thermoacoustics.*

[2] J. Wicker, W. Greene, S. Kim, Triggering of longitudinal combustion instabilities in rocket motors: Nonlinear combustion response, *Journal of Propulsion and Power* **12 (6)** (1996) 1148–1158.

[3] I. C. Waugh, M. P. Juniper, Triggering in a thermoacoustic system with stochastic noise, *Journal of Spray and Combustion Dynamics* **3 (3)**.

[4] K. Cliffe, A. Spence, S. Tavener, The numerical analysis of bifurcation problems with application to fluid mechanics, *Acta Numerica* **9 (00)** (2000) 39–131.

[5] J. Sánchez, F. Marques, J. M. Lopez, A Continuation and Bifurcation Technique for Navier-Stokes Flows, *Journal of Computational Physics* **180 (1)** (2002) 78–98.

[6] J. Sánchez, M. Net, B. García-Archilla, C. Simó, Newton-Krylov continuation of periodic orbits for Navier-Stokes flows, *Journal of Computational Physics* **201 (1)** (2004) 13–33.

[7] D. Viswanath, Recurrent motions within plane Couette turbulence, *Journal of Fluid Mechanics* **580** (2007) 339.

[8] C. C. Jahnke, F. E. C. Culick, Applicaiton of Dynamical Systems Theory to Nonlinear Combustion Instabilities, *Journal of Propulsion and Power* **10 (4)** (1994) 508–517.

[9] M. P. Juniper, Triggering in the horizontal Rijke tube: non-normality, transient growth and bypass transition, *Journal of Fluid Mechanics* **667** (2010) 272–308.

[10] P. Subramanian, S. Mariappan, R. I. Sujith, P. Wahi, Bifurcation analysis of thermoacoustic instability in a horizontal Rijke tube, *International Journal of Spray and Combustion Dynamics* **2 (4)** (2010) 325–355.

[11] D. Roose, K. Lust, A. Champneys, A. Spence, A Newton-Picard Shooting Method for Computing Periodic Solutions of Large-scale Dynamical Systems, *Chaos, Solitons & Fractals* **5 (10)** (1995) 1913–1925.

[12] Y. Saad, M. Schultz, GMRES: A generalized minimal residual algorithm for solving nonsymmetric linear systems., *SIAM J. Sci. Stat. Comput.* **7 (3)** (1986) 856–869.

[13] M. Tyagi, S. Chakravarthy, Unsteady combustion response of a ducted non-premixed flame and acoustic coupling, *Combustion Theory and Modelling* **11 (2)** (2007) 205–226.

[14] K. Balasubramanian, R. I. Sujith, Non-normality and nonlinearity in combustion-acoustic interaction in diffusion flames, *Journal of Fluid Mechanics* **594** (2008) 29–57.

[15] T. Poinsot, *Theoretical and numerical combustion*, 2nd Edition, R T Edwards, 2005.

[16] I. Waugh, S. Illingworth, M. P. Juniper, Matrix-free continuation for bifurcation analysis of large thermoacoustic systems, *Submitted to Journal of Computational Physics*, 2012.

[17] S. Illingworth, I. Waugh, M. P. Juniper, Finding thermoacoustic limit cycles for a ducted Burke-Schumann flame, *Submitted to Proceedings of the Combustion Institute*, 2012